

# Accepted Manuscript

Identification of unknown parameters of a single diode photovoltaic model using particle swarm optimization with binary constraints

Sangram Bana, R.P. Saini

PII: S0960-1481(16)30874-6

DOI: [10.1016/j.renene.2016.10.010](https://doi.org/10.1016/j.renene.2016.10.010)

Reference: RENE 8198

To appear in: *Renewable Energy*

Received Date: 31 March 2016

Revised Date: 13 August 2016

Accepted Date: 4 October 2016

Please cite this article as: Bana S, Saini RP, Identification of unknown parameters of a single diode photovoltaic model using particle swarm optimization with binary constraints, *Renewable Energy* (2016), doi: 10.1016/j.renene.2016.10.010.

This is a PDF file of an unedited manuscript that has been accepted for publication. As a service to our customers we are providing this early version of the manuscript. The manuscript will undergo copyediting, typesetting, and review of the resulting proof before it is published in its final form. Please note that during the production process errors may be discovered which could affect the content, and all legal disclaimers that apply to the journal pertain.



# 1 Identification of Unknown Parameters of a Single Diode 2 Photovoltaic Model Using Particle Swarm Optimization 3 with Binary constraints

4 \*SangramBana, R.P Saini  
5 \*Research Scholar, Professor

6 Alternate Hydro Energy Centre, Indian Institute of Technology, Roorkee-247667, India.  
7  
8  
9

10 **Abstract-Photo-voltaic (PV) is a static medium to convert solar energy directly into**  
11 **electricity. In order to predict the performance of a PV system before being installed, a**  
12 **reliable and accurate model design of PV systems is essential. To validate the design of a**  
13 **PV system like maximum power point (MPP) and micro-grid system through simulation,**  
14 **an accurate solar PV model is required. However, information provided by manufacturers**  
15 **in data sheets is not sufficient for simulating the characteristic of a PV module under**  
16 **normal as well as under diverse environmental conditions. In this paper, a particle swarm**  
17 **optimization (PSO) technique with binary constraints has been presented to identify the**  
18 **unknown parameters of a single diode model of solar PV module. Multi-crystalline and**  
19 **mono-crystalline technologies based PV modules are considered under the present study.**  
20 **Based on the results obtained, it has been found that PSO algorithm yields a high value of**  
21 **accuracy irrespective of temperature variations.**

22 **Keywords -Photovoltaic (PV) model, maximum power point (MPP), binary constraints,**  
23 **particle swarm optimization (PSO).**

24 \*Corresponding author. Tel.: +91 9758352972, E-mail address: [sonamdah@iitr.ac.in](mailto:sonamdah@iitr.ac.in) (Sangram Bana)  
25  
26  
27  
28  
29  
30  
31  
32



<i>Abbreviations</i>	
<i>ABSO</i>	Artificial Bee Swarm optimization
<i>BFA</i>	Bacteria foraging algorithm
<i>CPSTO</i>	Chaos particle swarm optimization algorithm
<i>CSA</i>	Cuckoo Search algorithm
<i>EAs</i>	Evolutionary algorithms
<i>GA</i>	Genetic algorithm
<i>MAE</i>	Mean absolute error
<i>MPP</i>	Maximum power point
<i>MPPT</i>	Maximum power point tracking
<i>PSO</i>	Particle swarm optimization
<i>PV</i>	Photo-voltaic
<i>RMSE</i>	Root mean square error
<i>SA</i>	Simulated annealing
<i>STC</i>	Standard test conditions

34

## 35 1. Introduction

36 In the current scenario, socio-economic development and human welfare around the  
 37 world depends on energy. Fossil fuels account maximum share in the overall generation.  
 38 However, carbon emissions and depletion are some issues associated with the use of fossil fuels.  
 39 The energy demand around the world is continuously increasing. If this escalating demand is to  
 40 be met with fossil fuels, the extensive use of fossil fuels will release a large amount of CO<sub>2</sub> and  
 41 other greenhouse gases. Renewable energy sources on the other hand are abundant in nature and  
 42 contain quite low or no greenhouse-gas emissions. Therefore, it is the necessity of today's world  
 43 to concentrate on renewable energy sources for electricity generation. Solar energy has been a  
 44 paramount part of renewable energy sources as it is available directly from the sun, whereas  
 45 wind, wave, hydro etc. are indirectly derived. Solar energy is also available in abundance and is  
 46 non exhaustible, but the technology to harness solar energy is still improving. Solar PV  
 47 technology exploits the solar radiation and directly converts it into electricity. The utilization of  
 48 photovoltaic (PV) technology as a source of power at user end is increasing, due to easy  
 49 implementation and low maintenance cost compared to other forms of energy conversion [1]. PV



78 The previous studies suggested that ideal model is simple but less accurate. Researchers  
79 in [10, 15-18] proposed models with four parameters ( $a, R_s, I_o, I_{pv}$ ) accounting shunt resistance to  
80 be infinite. Although, the proposed four parameters model has not been proved accurate yet, it is  
81 considered to be favorable as the unknown parameters can be easily identified in comparison to  
82 the model with five parameters ( $a, R_s, R_p, I_o$  and  $I_{pv}$ ).

83 To resolve the issue with the necessity of obtaining unknown parameters, a five  
84 parameter model based on the values of manufacturer datasheet was presented by Villalva et al.  
85 [19]. Value of ideality factor was obtained through trial and error method. The new value of  $R_s$   
86 and  $R_p$  depends upon the previous value of  $R_s$ . The new set of values was determined by  
87 continuously increasing  $R_s$  and simultaneously computing  $R_p$ . These values were determined till  
88 MPP of the presented model reaches to the same value as provided in manufacturer's datasheet  
89 at STC. Once unknown parameters are extracted, these parameters are fixed and again calculated  
90 for same model under the influence of varying insolation and temperature levels. Under standard  
91 test conditions (STC), the developed method yields accurate MPP. However accuracy gets  
92 compromised under the effect of varying temperature [20].

93 W. Xiao et al. [21] used a database of MPP acquired from manufacturer in order to  
94 produce exact MPP at varying temperatures. At different values of temperature, MPP was  
95 matched by regulating ideality factor through iterative technique. The drawback associated  
96 herewith is to obtain the availability of MPP for varying temperatures, which is not provided in  
97 manufacturer datasheet. Park and Choi [22] employed a parameter extraction method based on  
98 datasheet values. MPP error formulation is incorporated as objective function and parameter  
99 optimization is achieved by using pattern search algorithm.

100 Recently numerous evolutionary algorithms (EAs) were adopted to determine unknown  
101 parameters of a PV module under consideration. Jena and Ramana [23] presented a critical  
102 review based on modeling and parameter identification of a PV cell for simulation. They have  
103 analyzed  $R_s, R_p$  and two diode model along with different parameter identification schemes  
104 (analytical as well as soft computing). In recent years, the metaheuristic optimization algorithms  
105 such as genetic algorithm (GA) [24-26], simulated annealing (SA) [27], artificial Bee Swarm  
106 optimization (ABSO) algorithm [28, 29], and particle swarm optimization (PSO) [30], have

107 received considerable attention towards solar cell parameters identification problem.  
108 Metaheuristic algorithms are appropriate selections for resolving the drawback associated with  
109 parameter extraction at varying atmospheric conditions.

110 In case of GA, serious shortcomings, namely low speed and degradation for highly  
111 interactive fitness function has been reported [31, 32]. El-Naggar et al. [27] employed Simulated  
112 Annealing (SA) to extract the parameters of single and two-diode models for cell and module.  
113 The trade-off between the cooling schedule and initial temperature is the major issue that makes  
114 SA a less preferable choice. Jieming et al. [33] utilized Cuckoo Search algorithm (CSA) to  
115 identify the parameters of the conventional and an advanced form of the single diode model for  
116 PV cell and module. Askarzadeh and Rezazadeh [34] employed ABSO to obtain the parameters  
117 of the single and double-diode models for PV module. Rajasekar et al. [35] presented a Bacteria  
118 Foraging algorithm (BFA) to compute all parameters of the single diode  $R_p$ -model under varying  
119 operating temperature and insolation values. By utilizing parameters provided on the  
120 manufacturer's datasheet,  $I_{pv}$  and  $I_0$  were analytically computed, whereas  $a$ ,  $R_s$ , and  $R_p$  were  
121 obtained by optimizing equation of slope at MPP.

122 Qin and Kimball [36] eliminated the idea of unknown parameters estimation for the SPV  
123 model. They exploited the field test data along with PSO algorithm to determine the value of  $a$ ,  
124  $R_s$  and  $R_p$ . Measurements of short circuit current and load data were required for the field test.  
125 Hengsi and Jonathan [30] employed PSO to extract PV cell parameters from the data measured  
126 under real operating conditions of varying insolation and temperature. Wei H et al. [37] used  
127 chaos particle swarm optimization algorithm (CPSO) to obtain unknown parameters of the single  
128 diode  $R_p$  model for a module. In CPSO, the chaotic search mechanism is utilized to re-initiate the  
129 stationary particles-causing an enhanced local and global search capability. Ye et al. [38] utilized  
130 PSO to determine the cell parameters of the single and two-diode models from the I-V curves. In  
131 comparison to GA, PSO was found to be more accurate with better computational speed. On the  
132 basis of operating conditions, module technology and type of model researchers have employed  
133 numerous parameter extraction techniques having advantages and disadvantages of their own.  
134 Among all the techniques, performance of PSO algorithm is found to have an adequate sense of  
135 balance between accuracy, speed and complexity.

136 The PSO algorithm is a swarm intelligence optimization algorithm based on observations  
137 of the social behavior of bird flocking or fish schooling [28-30, 36-41]. Several authors have  
138 utilized and improved many versions of PSO algorithm [28,29,38-41]. However, every version  
139 of PSO has different advantage for different complex optimal problem. The major disadvantages  
140 observed in PSO are of premature convergence and the loss of diversity in the population.

141 In order to eliminate the mentioned disadvantage, a novel technique has been presented in  
142 this study to compute the unknown parameters ( $a$ ,  $R_s$  and  $R_p$ ) of a single diode PV model. In the  
143 present study, a PSO based single diode model is developed to predict unknown parameters  
144 under varying operating conditions. In order to retain these parameters within realistic ranges and  
145 considering the effects of temperature variation, a binary constraint has been imposed i.e. by  
146 penalizing the objective function when the solution attempts to exceed the predefined parameters  
147 boundary limits. The accuracy of the model is assured irrespective of the temperature change.

148 The present study deals with identification of PV model using PSO with binary  
149 constraints. An overview of mathematical modeling framework of a PV model is presented and  
150 further, the problem formulation along with the proposed optimization technique is discussed.  
151 Results and performance validation of the proposed technique are discussed in detail. Further,  
152 the obtained results are compared with the results of other methods proposed in [16] and [19].  
153 The proposed technique is found to be advantageous as it has the capability of determining  
154 ideality factor, series and shunt resistance simultaneously without the need of estimating ideality  
155 factor and field data measurements. Also, the extracted parameters are computed as a function of  
156 insolation and temperature.

157

## 158 **2. Mathematical Modeling framework of a PV module based on single diode model.**

### 159 *2.1. Ideal PV cell model*

160 An ideal PV cell is represented by photo-generated current ( $I_{pv}$ ) which diverges from the ideal  
161 outcome due to electrical and optical losses [23, 41]. Further, the effect of series and parallel  
162 resistance are not considered in this simplest PV model. Schematic for an ideal PV model is



163 shown earlier in Figure 1. Terminal current of an ideal model is represented by I-V  
 164 characteristics and mathematically expressed as:

$$165 \quad I = I_{pv} - I_d \quad (1)$$

166 The diode current ( $I_d$ ) signifies diffusion and recombination current in quasi steady state  
 167 regions of emitter and excess concentration regions of PN junction. This diode current is  
 168 represented by Shockley equation as:

$$169 \quad I_d = I_0 \{ e^{qV_d/aKT} - 1 \} \quad (2)$$

170 where  $q$  is the charge of an electron ( $1.6 \times 10^{-19} \text{C}$ ),  $K$  is the Boltzmann constant ( $1.3805 \times 10^{-23} \text{ J/K}$ )  
 171  $T$  is temperature (K),  $I_0$  is leakage current and  $V_d$  is the diode voltage.

172 The ideal mathematical model based on diode equation of Shockley and Queisser is  
 173 expressed as:

$$174 \quad I = I_{pv} - I_0 (e^{qV_d/aKT} - 1) \quad (3)$$

175 Ideal solar PV cell does not consider the effect of internal resistance, thus fails to  
 176 establish an accurate relationship between cell current and voltage.

## 177 2.2. Practical PV cell Model.

178 In order to achieve accurate results, a series resistance is introduced to the ideal PV cell  
 179 model. Although this model is simple but it reveals deficiencies when subjected to temperature  
 180 variations. To overcome this limitation, the model has been extended further by considering a  
 181 shunt resistance and is termed as Practical PV cell. Thus, the practical single diode PV or five  
 182 parameter ( $I_{pv}$ ,  $I_0$ ,  $a$ ,  $R_s$  and  $R_p$ ) model consists of current producer and a diode with series and  
 183 shunt resistance as shown in Fig. 2[4-12, 42]. The characteristics I-V curve of a practical PV cell  
 184 is shown in Fig. 3.

185

186

**Fig.2.** Equivalent circuit of a practical PV cell

187

188 **Fig.3.** I-V characteristics curve of a PV cell.

189 The series resistance signifies resistance (ohmic loss) offered to the current flow due to  
 190 ohmic contact (metal-semiconductor contact) and impurity concentrations along with junction  
 191 depth. Leakage current across the junction signifies shunt resistance, connected parallel to the  
 192 diode. The mathematical representation of terminal current in Eq. (1) is modified as:

$$193 \quad I = I_{pv} - I_d - V_d/R_p \quad (4)$$

$$194 \quad V_d = V + IR_s \quad (5)$$

195 where  $V$  is input voltage and  $I$  is the terminal current.

196 It is recognized that I-V characteristic curve of a PV cell is affected by both series  
 197 resistance and shunt resistance. The output voltage is affected by series resistance; while shunt  
 198 resistance is responsible for reduction in available current [14-15, 43-47].Eq. (3) is modified to  
 199 obtain the equation of single diode PV model. The terminal current of a single diode(five-  
 200 parameter) model is given by:

$$201 \quad I = I_{pv} - I_0 \left[ \exp \left( \frac{V+IR_s}{aV_t} \right) - 1 \right] - \frac{V+IR_s}{R_p} \quad (6)$$

202 where  $V_T$  is the thermal voltage ( $nkT/q$ ).

### 203 2.3. Modeling of a PV module

204 A PV module may consist of number of PV cells which can be connected in series or  
 205 parallel. This series-parallel topology is represented in Fig. 4.

206

207 **Fig.4.** Equivalent circuit model of a PV module

208 The parameters of a PV cell are transformed in order to represent a PV module. Table 1  
 209 represents the parameters which are transformed due to series/parallel PV topologies [45, 47].

210 Table 1: Transformed parameters for series and parallel topologies.

211 Terminal current for series-parallel configuration of a PV module can be written as;

$$I = N_p \left\{ I_{pv} - I_{s1} \left[ \exp \left( \frac{V + IR_s \left( \frac{N_s}{N_p} \right)}{a N_s V_t} \right) - 1 \right] \right\} - \frac{V + IR_s \left( \frac{N_s}{N_p} \right)}{R_{sh} \left( \frac{N_s}{N_p} \right)} \quad (7)$$

A single PV module is a particular case of PV cells connected in series. Therefore, the number of cells connected in series (i.e.  $N_s$ ) will be scaled with  $V_t$ . Now, equation (6) can be rewritten as;

$$I = I_{pv} - I_0 \left[ \exp \left( \frac{V + IR_s}{a N_s V_t} \right) - 1 \right] - \frac{V + IR_s}{R_p} \quad (8)$$

Depending upon the load requirements, the numbers of modules are connected in series to increase voltage levels, whereas modules are connected in parallel to increase current levels.

When the terminals of a PV module are short-circuited, the current that flows through the circuit is termed as short-circuit current ( $I_{sc}$ ). It is the maximum current that flows through a PV cell.  $I_{sc}$  of a PV module depends on incident insolation, which is determined by the spectrum of incident light, i.e. AM 1.5 spectrum.  $I_{sc}$  also depends on cell area and its ability to absorb incident solar radiation [23]. At a given temperature  $T$ ,  $V=0$  and  $I=I_{sc}$ , Eq.(8) becomes:

$$I_{sc}(T) = \frac{R_p}{R_s + R_p} \left\{ I_{pv} - I_0 \left[ \exp \left( \frac{I_{sc}(T) + R_s}{a N_s V_t(T)} \right) - 1 \right] \right\} \quad (9)$$

Open circuit voltage ( $V_{oc}$ ) is the maximum voltage that can be delivered by a PV module. The Open circuit voltage corresponds to forward bias voltage, at which dark current compensates the photo-generated current and  $V_{oc}$  is dependent on the density of photo-generated current. At open circuit condition  $I=0$ ,  $V=V_{oc}$  and Eq. (8) becomes;

$$V_{oc}(T) = R_p \left\{ I_{pv} - I_0 \left[ \exp \left( \frac{V_{oc}(T)}{a N_s V_t(T)} \right) - 1 \right] \right\} \quad (10)$$

At a given temperature, maximum power is determined by the product of maximum current and voltage as shown in Fig. 3. By substituting  $I=I_{mp}$  and  $V=V_{mp}$ , the maximum power at a given temperature can be determined from Eq. (8) as:

$$P_{mp}(T) = \frac{R_p V_{mp}(T)}{R_s + R_p} \times \left\{ I_{pv} - I_0 \left[ \exp \left( \frac{V_{mp}(T) + I_{mp}(T) R_s}{a N_s V_t(T)} \right) - 1 \right] - \frac{V_{mp}(T)}{R_p} \right\} \quad (11)$$

234 Equations (9-11) are the data points used by the optimizer to provide the finest set of  
 235 values for  $a$ ,  $R_p$  and  $R_s$ . Also, the proportional effect of insolation intensity ( $G$ ) and operating  
 236 temperature ( $T$ ) on the PV output current are given in Eqs. (9-11) [10, 13-15, 42-47].

237 The insolation dependence of PV current is given by;

$$238 \quad I_{pv}(G, T) = \frac{G}{G_n} (I_{pv,n} + K_{I_{sc}} \Delta T) \quad (12)$$

239 Where  $I_{pv,n}$  is PV current and  $G_n$  is the solar radiation intensity in  $W/m^2$  at STC under nominal  
 240 conditions,  $K_{I_{sc}}$  is the temperature coefficient of short circuit current ( $mA/^\circ C$ ) and  $\Delta T (=T-T_n)$  is  
 241 the difference of temperature between the present moment and STC.

#### 242 2.4. Effect of Temperature

243 Solar cells work best at low temperature as determined by their material  
 244 properties. The cell efficiency decreases as the temperature escalates above operating  
 245 temperature. A substantial part of incident insolation is lost in the form of heat resulting in high  
 246 temperature of cells. To determine the effect of temperature on maximum power,  $P_{mpp,e}(T)$ , open  
 247 circuit voltage,  $V_{oc,e}(T)$  and short circuit current,  $I_{sc,e}(T)$  at a given temperature are expressed as;

$$248 \quad I_{sc,e}(T) = I_{sc,n} + K_{I_{sc}} \Delta T \quad (13)$$

$$249 \quad V_{oc,e}(T) = V_{oc,n} + K_{V_{oc}} \Delta T \quad (14)$$

$$250 \quad P_{mp,e}(T) = P_{mp,n} + K_{P_{mp}} \Delta T \quad (15)$$

251 where  $P_{mpp,n}$ ,  $V_{oc,n}$  and  $I_{sc,n}$  respectively represents maximum power, open circuit voltage and  
 252 short circuit current under nominal circumstances.  $K_{V_{oc}}$  and  $K_{P_{mp}}$  are the temperature coefficient  
 253 of open circuit voltage and maximum power point provided by the manufacturers as shown in  
 254 Table 2. The datasheets of the considered modules are provided in Ref. [48], [49] and [50].

255

256

257

258



285 To normalize the objective function, the numerator and denominator of equations from  
 286 Eq. (21-23) are obtained from Eqs. (9-11) and (13-15), respectively. This ensures that the range  
 287 of the terms in the objective function is same.

$$288 \quad fI_{sc}(a, R_s, R_p, T) = \frac{I_{sc}(T)}{I_{sc,e}(T)} - 1 \quad (21)$$

$$289 \quad fV_{oc}(a, R_s, R_p, T) = \frac{V_{oc}(T)}{V_{oc,e}(T)} - 1 \quad (22)$$

$$291 \quad fP_{mp}(a, R_s, R_p, T) = \frac{P_{mp}(T)}{P_{mp,e}(T)} - 1 \quad (23)$$

### 293 3.2. Binary Constraints Handling Approach

294 PV modules' parameters like ideality factor, series resistance and parallel resistance must  
 295 be within their limits. Three set of constraints are imposed to handle this problem. The  
 296 constraints are expressed as:

$$297 \quad a_{\min} < a < a_{\max} \quad (24)$$

$$298 \quad R_{s,\min} < R_s < R_{s,\max} \quad (25)$$

$$299 \quad R_{p,\min} < R_p < R_{p,\max} \quad (26)$$

300 where the minimum and maximum values of the parameters to be determined are represented by  
 301 the subscripts 'min' and 'max', respectively. The binary constraints considered for simulation are  
 302 given in Table 3.

303 Table 3: Binary constraints considered for simulation

304 A binary constraint handling approach is proposed to penalize the objective function if  
 305 any of the above constraint violates. The proposed approach for handling binary constraints is  
 306 expressed as follows:

$$307 \quad f_{\text{barrier}} = [(sign(a_{\min} - a) + sign(a_{\max} - a))^2 + (sign(R_{s,\min} - R_s) + sign(R_{s,\max} - R_s))^2 + (sign(R_{p,\min} - R_p) + sign(R_{p,\max} - R_p))^2] \quad (27)$$

308 where sign(x) is a function return as -1, 0 and 1 if  $x < 0$ ,  $x = 0$  and  $x > 0$ , respectively. This  
 309 binary constraint handling approach is having advantages over the other constraints handling  
 310 approach as it only penalizes the objective function if there is a constraint violation.

311 By introducing binary constraint handling approach term into the objective function, i.e.,  
 312  $f_{obj} = |f_{Isc}| + |f_{Voc}| + |f_{Pmp}| + |f_{barrier}|$ , the problem is transformed into an unconstrained optimization  
 313 problem.

314 The objective function given by Eq. (20) is minimized in order to determine  $a$ ,  $R_s$  and  $R_p$   
 315 by formulating the PSO approach. In previous studies [37-39, 45-50], PSO algorithm based  
 316 technique has been used for maximization of the objective function. Whereas in the present  
 317 study, the objective function is minimized to zero for different values of temperature and  
 318 insolation using an absolute function.

### 319 3.3. PSO algorithm

320 Particle swarm optimization is inspired by social and cooperative behavior displayed by  
 321 various species to fill their needs in the search space. The algorithm is guided by personal  
 322 experience (Pbest), overall experience (Gbest) and the present movement of the particles to  
 323 decide their next positions in the search space. Further, the experiences are accelerated by two  
 324 factors  $c_1$  and  $c_2$  known as acceleration coefficients, and two random numbers generated between  
 325  $[0, 1]$ , whereas the present movement is multiplied by an inertia factor ' $\omega$ ' varying between  
 326  $[\omega_{min}, \omega_{max}]$ . The size of the population is considered as ' $N$ ' and the dimension of each element  
 327 of the population is considered as  $D$ , where  $D$  represents the total number of variables. The initial  
 328 solution is denoted as  $\mathbf{X} = [\mathbf{X}_1, \mathbf{X}_2, \dots, \mathbf{X}_N]^T$ , where ' $T$ ' denotes the transpose operator. Each  
 329 individual  $\mathbf{X}_i$  ( $i = 1, 2, \dots, N$ ) is given as  $\mathbf{X}_i = [X_{i,1}, X_{i,2}, \dots, X_{i,D}]$ . The initial velocity of the  
 330 population is denoted as  $\mathbf{V} = [\mathbf{V}_1, \mathbf{V}_2, \dots, \mathbf{V}_N]^T$ . Thus, the velocity of a particle  $\mathbf{X}_i$  ( $i = 1, 2, \dots, N$ )  
 331 is given as  $\mathbf{V}_i = [V_{i,1}, V_{i,2}, \dots, V_{i,D}]$ .

332 The flowchart of the proposed PSO-based inverse barrier technique is shown in Fig. 5.

333

334 **Fig.5.**Flowchart of the proposed technique

335 The different steps of PSO are as follows for  $\forall i$  and  $\forall j$  (where ' $i$ ' represents particle and ' $j$ '  
 336 its dimension):

337 Step 1. Set parameter  $\omega_{min}$ ,  $\omega_{max}$ ,  $c_1$  and  $c_2$  of PSO

- 338 Step 2. Initialize population of particles having positions  $\mathbf{X}$  and velocities  $\mathbf{V}$
- 339 Step 3. Set iteration  $k = 1$
- 340 Step 4. Calculate fitness of particles  $F_i^k = f(\mathbf{X}_i^k)$  and find the index of the best particle  $b$
- 341 Step 5. Select  $\mathbf{Pbest}_i^k = \mathbf{X}_i^k$  and  $\mathbf{Gbest}^k = \mathbf{X}_b^k$
- 342 Step 6. Take  $\omega = \omega_{max} - k \times (\omega_{max} - \omega_{min}) / \text{Max}_{iteration}$
- 343 Step 7. Update velocity and position of particles as;
- 344  $V_{ij}^{k+1} = w \times V_{ij}^k + c_1 \times \text{rand}(\ ) \times (\mathbf{Pbest}_{ij}^k - X_{ij}^k) + c_2 \times \text{rand}(\ ) \times (\mathbf{Gbest}_j^k - X_{ij}^k); \forall j \text{ and } \forall i$
- 345  $X_{ij}^{k+1} = X_{ij}^k + V_{ij}^{k+1}; \forall j \text{ and } \forall i$
- 346 Step 8. Evaluate fitness  $F_i^{k+1} = f(\mathbf{X}_i^{k+1})$  and find the index of the best particle  $b1$
- 347 Step 9. Update Pbest of population
- 348 If  $F_i^{k+1} < F_i^k$ , then,  $\mathbf{Pbest}_i^{k+1} = \mathbf{X}_i^{k+1}$ ; else  $\mathbf{Pbest}_i^{k+1} = \mathbf{Pbest}_i^k$ ;
- 349 Step 10. Update Gbest of population
- 350 If  $F_{b1}^{k+1} < F_b^k$  then  $\mathbf{Gbest}^{k+1} = \mathbf{Pbest}_{b1}^{k+1}$  and set  $b = b1$  else  $\mathbf{Gbest}^{k+1} = \mathbf{Gbest}^k$
- 351 Step 11. If  $k < \text{Maxite}$  then  $k = k + 1$  and go to step 6 else go to step 12
- 352 Step 12. Print optimum solution as  $\mathbf{Gbest}^k$

353 Based on the randomly generated population, the PSO technique provides a collection of  
 354 different solutions for  $a$ ,  $R_s$  and  $R_p$  with each new execution of the optimization technique. This  
 355 provides a set of I-V curves.

356 The technique provides several I-V and P-V curves as shown in Figure 6 and 7  
 357 respectively that meet the objective function to confirm the authentication of the presented  
 358 algorithm. The circle markers on these curves indicate  $[0, I_{sc}]$ ,  $[V_{mp}, I_{mp}]$  and  $[V_{oc}, 0]$  which are  
 359 the points that the I-V curve of the proposed method (indicated by the solid lines) must pass  
 360 through.

361

362

**Fig.6.** I-V curves obtained by the presented technique

363

364

**Fig.7** P-V curves obtained by the presented technique.



365 The overall model error defined for each set of curves in Figure 6 and 7 is represented by  
 366 the following equation;

$$367 \quad \varepsilon_i = |P_{mp,m_i}(T) - P_{mp,e}(T)| + |V_{mp,m_i}(T) - V_{mp,e}(T)| \quad (28)$$

368 Where  $\varepsilon$  is the overall model error and subscript  $i$  signifies the specific curve under assessment.  
 369 From all the possible optimized solution, outcome with the least value of  $\varepsilon$  is selected as the best  
 370 solution.

#### 371 4. Results and Discussions

372 Performance of the proposed optimization technique (PSO approach) has been investigated  
 373 first. The parameters such as population size ' $ps$ ' and acceleration coefficients  $c_1$  and  $c_2$  affect the  
 374 execution of PSO. MATLAB environment is used to conduct this mathematical study. The  
 375 parameters set up for considered PSO algorithm is shown in Table 4:

376 Table 4: Parameters setup for considered PSO algorithm

##### 377 4.1. Convergence of PSO

378 In order to study the convergence of PSO for the proposed technique, PV modules of two  
 379 different technologies have been used. As the temperature varies, for each value of temperature,  
 380 PSO is implemented and gets terminated after 1000 generations. The optimization has been  
 381 repeated for 100 times with some new sets of population in order to achieve the average of  
 382 optimized results. Figure 8 shows the best fitness value versus generations plot for different  
 383 values of temperature.

384  
 385 **Fig.8.** Best fitness versus generations for  $T=0^{\circ}\text{C}$  to  $75^{\circ}\text{C}$  for Shell SQ85

386 The fitness value in curves converges to zero for SQ85 PV module irrelevant of the operating  
 387 temperature. Similar results can be achieved for KD210GH-2PU and SP70 PV module. It is  
 388 observed that after every 100 generations the fitness value drops down to zero in 8ms of time to  
 389 confirm the convergence of the fitness value.

##### 390 4.2. Model validation

391 Based on the convergence of the proposed algorithm, the PV modules of two different  
392 technologies are used to evaluate the proposed model under the present study. The parameters  
393 and constraints of these technologies are specified earlier in Tables 2 and 3, respectively. The  
394 identified parameters obtained by applying the proposed optimization technique are presented in  
395 Figure 9.

396  
397 **Fig.9.** Model parameters for KD210GH-2PU, SP70 and SQ85 at 0°C to 75°C. (a) Ideality factor. (b) Series  
398 resistance. (c) Shunt resistance.

399 Ideality factor, series resistance and shunt resistance for two different technologies  
400 (Mono-crystalline, KD210GH-2PU and Poly-crystalline, SP70 and SQ85 PV modules) have  
401 been extracted by the proposed technique for different values of temperature in the range of T =  
402 0°C to 75°C. Parameters exhibit non-linear characteristics and the ideality factor is on an urge of  
403 decrease [Figure 9(a)]. On the other hand, series resistance shows escalating tendency [Figure 9  
404 (b)] for SP70 and SQ85 PV modules. However, KD210GH-2PU PV module indicates the  
405 declining tendency in series resistance and inclining trend in ideality factor with increase in  
406 temperature. In case of shunt resistance, the values identified approximately remains constant for  
407 KD210GH-2PU, SP70 and SQ85 PV modules. Series resistance decreases with increase in the  
408 ideality factor and vice-versa. However, a slight variation has been observed in case of shunt  
409 resistance.

410 Out of 100 independent runs, the best value, mean value and worst value of ideality  
411 factor, series resistance and shunt resistance at different temperatures for KD210GH-2PU and  
412 SQ85 PV modules are presented in Table 5.

413 Table 5: Identified parameters for KD210GH-2PU and SQ85 PV modules

414 Based on the obtained values of the unknown parameters, I-V and P-V curves of  
415 KD210GH-2PU PV module at different insolation and temperature are obtained as shown in  
416 Figure 10 and Figure 11 respectively.

417

418 **Fig.10.** I–V and P–V curves of proposed model (solid line) and manufacturer’s experimental data (circle marker at  
 419  $I_{sc}$ ,  $P_{mp}$  and  $V_{oc}$ ) of KD210GH-2PU (Multi-crystalline) PV module under different irradiation,  $T = 25^{\circ}\text{C}$ .

420

421 **Fig.11.** I–V and P–V curves of proposed model (solid line) and manufacturer’s experimental data (circle marker at  
 422  $I_{sc}$ ,  $P_{mp}$  and  $V_{oc}$ ) of KD210GH-2PU (Multi-crystalline) PV module at different temperature,  $G = 1000\text{W}/\text{m}^2$ .

423 The circle marker at  $I_{sc}$ ,  $P_{mp}$  and  $V_{oc}$  indicates manufacturer’s experimental data and the  
 424 results based on the proposed method are indicated by the solid lines. So, the proposed  
 425 methodology and obtained results clearly indicate that the achieved characteristic curves are  
 426 quite similar to the manufacturer’s data, irrespective of varying atmospheric conditions.

#### 427 4.3 Comparison of the proposed technique

428 In order to keep point of reference of the proposed technique with techniques used in [16]  
 429 and [19], the relation between absolute error in power and voltage is shown in Figure 12. It is  
 430 seen that a similar range of accuracy is obtained between the presented method and method used  
 431 in [19] for different values of temperature. The proposed method offers better accuracy at MPP,  
 432 whereas, the method presented in [16], shows a considerable amount of error for different values  
 433 of temperature.

434

435 **Fig.12.** Absolute power error for KD210GH-2PU (Multi-crystalline) at (a)  $T = 25^{\circ}\text{C}$ , (b)  $T = 50^{\circ}\text{C}$ , and (c)  $T =$   
 436  $75^{\circ}\text{C}$ ,  $G = 1000\text{W}/\text{m}^2$ , A.M = 1.5.

437 By making the variations of  $1^{\circ}\text{C}$  in the range of temperature from  $0^{\circ}\text{C}$  to  $75^{\circ}\text{C}$ , the  
 438 findings based on two other PV modules (SP70 and SQ85) have also been observed. Figure 13  
 439 illustrates the average result of SP70 PV module for 100 data sets.

440

441 **Fig.13.** Absolute error at MPP for SP-70 (Mono-crystalline) at different temperature,  $G=1000\text{ W}/\text{m}^2$ , A.M =1.5.

442 Under STC, the error in results illustrated by model [19] is 0.013% for  $P_{mp}$  and 0.0515%  
 443 for  $V_{mp}$  at MPP. As the temperature deviates from STC, accuracy decreases up to 2.73% and  
 444 2.11% at  $0^{\circ}\text{C}$  and  $75^{\circ}\text{C}$  temperature, respectively. Also variation of error in  $V_{mp}$  is observed at  
 445  $0^{\circ}\text{C}$  to  $75^{\circ}\text{C}$  (mean=0.573% and standard deviation=0.289%).

446 In the present study, error of 0.001% for ' $P_{mp}$ ' and 0.10% for  $V_{mp}$  at STC are found. The  
447 maximum error 0.011% for  $P_{mp}$  is observed for specified temperature range and a standard  
448 deviation of 0.045 for  $V_{mp}$  is obtained. The obtained value is six times lower as compared to [19].  
449 A similar pattern of results is obtained for SQ85 PV module. Table 6 gives the mean and  
450 standard deviation values for SP70 and SQ85 PV modules.

451 Table 6: Comparison of absolute error at MPP (A.M 1.5, 1000 W/m<sup>2</sup>)

452 It is therefore recommended that in order to attain low modeling error under temperature  
453 variation, it is essential to adjust  $a$ ,  $R_s$  and  $R_p$ .

## 454 5. Conclusions and future works

455 A novel approach of optimization technique based on PSO with binary constraints is  
456 presented in order to identify the unknown parameters of a single diode model. The proposed  
457 method completely eliminates the requirement of assuming the ideality factor. It also includes  
458 the temperature variations to identify the unknown parameters.

459 The evaluation of three different PV modules ensures the robustness of the proposed  
460 technique. The two novel approaches have been considered as a point of reference for the  
461 proposed technique. Appreciable accuracy in the results is achieved irrespective of temperature  
462 variations. The PSO algorithm has been executed 100 times with same initial condition as well as  
463 with standard parameter values provided by the manufacturer. The mean of maximum modeling  
464 error at MPP is found to be less than 0.02 % for maximum voltage and 0.26 % for maximum  
465 power.

466 In future, following works are proposed to improve the performance of PV model:

- 467 • With growing interests in the study of partial shading and accuracy concerns associated with  
468 low insolation and large PV installations, performance prediction is important for accurate  
469 energy yield. More elaborate and accurate models like two-diode model (or three-diode  
470 model) must be incorporated for performance analysis of the PV system.
- 471 • Further, one of the promising alternatives for computing the model parameters under these  
472 conditions could be hybrid approach.

- 473 • Furthermore, the PV models are still based on mono-crystalline and poly-crystalline  
474 technology. For instance, amorphous thin film modules have high ideality factor due to low  
475 fill factors. However, models presume fill factor in the range of  $1 < a < 2$ . There are very few  
476 committed efforts carried out for multi-junction, organic and dye synthesized PV cells. These  
477 are emerging areas of interests and particular problems related to them must be resolved.
- 478 • Finally, problems associated to cell degradations with time and weather conditions must be  
479 addressed. Additional coefficients can be added to mimic the cell deterioration for different  
480 module technologies. This effort will offer a greater understanding of the module  
481 performance over an extensive period of time.

### 482 Acknowledgement

483 This work was supported by Grant of Ministry of New and Renewable Energy (MNRE),  
484 Government of India (8793-38-061/429) and Indian Institute of Technology (IIT) Roorkee,  
485 Uttarakhand, India.

### 486 REFERENCES

- 487
- 488 [1] Oliva D, Cuevas E, Pajares G, 2014. Parameter identification of solar cells using artificial  
489 bee colony optimization. *Energy*, 72:93–102.
- 490 [2] Energy at the crossroads; 2015. ([http://home.cc.umanitoba.ca/~vsmil/pdf\\_pubs/oecd.pdf](http://home.cc.umanitoba.ca/~vsmil/pdf_pubs/oecd.pdf)).
- 491 [3] Buresch M, *Photovoltaic Energy System: Design and Installation*. New York: McGraw-  
492 Hill, 1983, p. 335.
- 493 [4] Soon T. Kok and MekhilefSaad, 2015. "A Fast-converging MPPT Technique for  
494 Photovoltaic System under Fast Varying Solar Irradiation and Load Resistance," *IEEE*  
495 *Transactions on Industrial Informatics*, Vol.11, Issue 1, pp. 176- 186.
- 496 [5] Weidong X, Dunford WG, Capel A. A novel modeling method for photovoltaic cells. In:  
497 35th Annual power electronics specialists conference, 2004, PESC 04 2004, vol. 3. IEEE;  
498 2004. p. 1950–6.
- 499 [6] Ulapane NNB, Dhanapala CH, Wickramasinghe SM, Abeyratne SG, Rathnayake N,  
500 Binduhewa PJ. Extraction of parameters for simulating photovoltaic panels. In: 6th IEEE  
501 international conference on industrial and information systems (ICIIS), 2011; 2011. p. 539–  
502 44.

- 503 [7] Chenni R, Makhlof M, Kerbache T, Bouzid A. A detailed modeling method for  
504 photovoltaic cells. *Energy* 2007; 32:1724–30.
- 505 [8] Kou Q, Klein SA, Beckman WA. A method for estimating the long-term performance of  
506 direct-coupled PV pumping systems. *Solar Energy* 1998; 64:33–40.
- 507 [9] Bellini A, Bifaretti S, Iacovone V, Cornaro C. Simplified model of a photovoltaic module.  
508 In: *Applied electronics, 2009 AE 2009. IEEE; 2009.* p. 47–51.
- 509 [10] Moran C. G, Arbolea P, Reigosa D, Diaz G, and Aleixandre J. G, “Improved model of  
510 photovoltaic sources considering ambient temperature and solar irradiation,” in *Proc. IEEE*  
511 *PES/IAS Conf. Sustainable Alternative Energy, 2009*, pp. 1–6.
- 512 [11] Kun D, XinGao B, HaiHao L, Tao P. A MATLAB-Simulink-Based PV module model and  
513 its application under conditions of non-uniform irradiance. *IEEE Trans Energy Convers*  
514 *2012; 27:864–72.*
- 515 [12] Humada A. M, Hojabri M, Mekhilef S, Hamada H M, 2016. “Solar cell parameters  
516 extraction based on single and double-diode models: A review”. *Renewable and*  
517 *Sustainable Energy Reviews* 56 494–509.
- 518 [13] Kajihara and Harakawa T, “Model of photovoltaic cell circuits under partial shading,” in  
519 *Proc. IEEE Int. Conf. Ind. Technol., 2005*, pp. 866–870.
- 520 [14] Tan Y. T, Kirschen D. S, and Jenkins N, “A model of PV generation suitable for stability  
521 analysis,” *IEEE Trans. Energy Convers.*, vol. 19, no. 4, pp. 748–755, Dec. 2004.
- 522 [15] Altas H and Sharaf A. M, “A photovoltaic array simulation model for MATLAB-simulink  
523 GUI environment,” in *Proc. Int. Conf. Clean Elect. Power, 2007*, pp. 341–345.
- 524 [16] Matagne E, Chenni R, and Bachtiri R. El, “A photovoltaic cell model based on nominal  
525 data only,” in *Proc. Int. Conf. Power Eng., Energy Elect. Drives, 2007*, pp. 562–565.
- 526 [17] Xiao W, Dunford W. G, and Capel A, “A novel modeling method for photovoltaic cells,”  
527 in *Proc. IEEE 35th Annu. Power Electron. Spec. Conf., 2004*, vol. 3, pp. 1950–1956.
- 528 [18] Walker G, “Evaluating MPPT converter topologies using a MATLAB PV model,” *J. Elect.*  
529 *Electron. Eng. Aust.*, vol. 21, no. 1, pp. 45–55, 2001.
- 530 [19] Villalva M. G, Gazoli J. R, and Filho E. R, “Comprehensive approach to modeling and  
531 simulation of photovoltaic arrays,” *IEEE Trans. Power Electron.*, vol. 24, no. 5, pp. 1198–  
532 1208, May 2009.

- 533 [20] Bashahu M and Nkundabakura P, “Review and tests of methods for the determination of  
534 the solar cell junction ideality factors,” *Sol. Energy*, vol. 81, pp. 856–863, 2007.
- 535 [21] Al-Awami A. T, Zerguine A, Cheded L, Zidouri A, and Saif W, “A new modified particle  
536 swarm optimization algorithm for adaptive equalization,” *Digital Signal Processing*, vol.  
537 21, no. 2, pp. 195–207, Mar. 2011.
- 538 [22] Park J.Y., Choi S.J., 2015. A novel datasheet-based parameter extraction method for a  
539 single-diode photovoltaic array model. *Solar Energy* 122; 1235–1244.
- 540 [23] Jena D, Ramana V. R, 2015. Modeling of photovoltaic system for uniform and non-  
541 uniform irradiance: A critical review *Renewable and Sustainable Energy Reviews* 52, 400–  
542 417.
- 543 [24] Maherchandani J. K, Agarwal C, and Sahi M, “Estimation of Solar Cell Model Parameter  
544 by Hybrid Genetic Algorithm Using MATLAB,” *International Journal of Advanced*  
545 *Research in Computer Engineering & Technology*, vol. 1, no. 6, pp. 78–81, 2012.
- 546 [25] Zagrouba M, Sellami A, Boua M, and Ksouri M, “Identification of PV solar cells and  
547 modules parameters using the genetic algorithms: Application to maximum power  
548 extraction,” *Solar Energy*, vol. 84, pp. 860–866, 2010.
- 549 [26] Patel S. J, Panchal A. K, and Kheraj V, “Solar Cell Parameters Extraction from a Current-  
550 Voltage Characteristic Using Genetic Algorithm,” *Journal of Nano and Electronic Physic*,  
551 vol. 5, no. 2, pp. 5–7, 2013.
- 552 [27] El-Naggar KM, Al-Rashidi MR, Al-Hajri MF, Al-Othman AK., 2012. Simulated annealing  
553 algorithm for photovoltaic parameters identification. *Solar Energy*; 86:266–74.
- 554 [28] Shi Y and Eberhart R, “Parameter selection in particle swarm optimization,” in in  
555 *Evolutionary Programming VII SE - 57*, vol. 1447, V. W. Porto, N. Saravanan, D. Waagen,  
556 and A. E. Eiben, Eds. Springer Berlin Heidelberg, 1998, pp. 591–600.
- 557 [29] Khare A and Rangnekar S, “A review of particle swarm optimization and its applications in  
558 Solar Photovoltaic system,” *Applied Soft Computing Journal*, vol. 13, no. 5, pp. 2997–  
559 3006, 2013
- 560 [30] Hengsi Q, Kimball JW. 2011. Parameter determination of photovoltaic cells from field  
561 testing data using particle swarm optimization. In: *Power and energy conference at Illinois*  
562 (PECI), 2011. IEEE;. p. 1–4.

- 563 [31] Ji M, Jin Z, Tang H. An improved simulated annealing for solving the linear constrained  
564 optimization problems. *Appl Math Comput* 2006; 183:251–9.
- 565 [32] Zwe-Lee G. A particle swarm optimization approach for optimum design of PID controller  
566 in AVR system. *IEEE Trans Energy Convers* 2004; 19:384–91.
- 567 [33] Ma J, Ting TO, Man KL, Zhang N, Guan S-U, Wong PWH, 2013. Parameter estimation of  
568 photovoltaic models via cuckoo search. *J Appl Math*; 2013:8.
- 569 [34] Askarzadeh A. and Rezazadeh A., “Artificial bee swarm optimization algorithm for  
570 parameters identification of solar cell models,” *Applied Energy*, vol. 102, pp. 943–949,  
571 2013.
- 572 [35] Rajasekar N, Kumar NK, Venugopalan R., 2013. Bacterial foraging algorithm based solar  
573 PV parameter estimation. *Solar Energy*; 97:255–65.
- 574 [36] Qin H and Kimball J. W., “Parameter determination of photovoltaic cells from field testing  
575 data using particle swarm optimization,” in *Proc. IEEE Power Energy Conf.*, 2011, pp. 1–4.
- 576 [37] Wei H, Cong J, Lingyun X, Deyun S. Extracting solar cell model parameters based on  
577 chaos particle swarm algorithm. In: *2011 International conference on electric information  
578 and control engineering (ICEICE)*. IEEE; p. 398–402.
- 579 [38] Ye M, Wang X, Xu Y., 2009. Parameter extraction of solar cells using particle swarm  
580 optimization. *J Appl Phys*; 105:094502.
- 581 [39] Chun-man Y A. N, Bao-long G. U. O, and Xian-xiang W. U, “Empirical Study of the  
582 Inertia Weight Particle Swarm Optimization with Constraint Factor,” *International Journal  
583 of Soft Computing And Software Engineering*, vol. 2, no. 2, pp. 1– 8, 2012.
- 584 [40] Liang X, Yin Z, Wang Y, and Sun Q, “Impulse Engine Ignition Algorithm Based on  
585 Genetic Particle Swarm Optimization,” in *Advances in Swarm Intelligence SE - 5*, vol.  
586 7929, Y. Tan, Y. Shi, and H. Mo, Eds. Springer Berlin Heidelberg, 2013, pp. 35–43.
- 587 [41] Bellia H, Ramdani Y, Moulay F. A detailed modeling of photovoltaic module using  
588 MATLAB. *NRIAG Journal of Astronomy and Geophysics* (2014) 3, 53–61.
- 589 [42] Alain K. Tossa, Y.M. Soro, Y. Azoumah, D. Yamegueu, 2014. A new approach to estimate  
590 the performance and energy productivity of photovoltaic modules in real operating  
591 conditions. *Sol. Energy* 110 543-560.
- 592 [43] Xiao W, Dunford W. G, and Capel A, “A novel modeling method for photovoltaic cells,”  
593 in *Proc. IEEE 35th Annu. Power Electron. Spec. Conf.*, 2004, vol. 3, pp. 1950–1956.



- 594 [44] DhiaaHalbootMuhsen, Abu Bakar Ghazali, Tamer Khatib, Issa Ahmed Abed, (2016). A  
595 comparative study of evolutionary algorithms and adapting control parameters for  
596 estimating the parameters of a single-diode photovoltaic module's model. Renewable  
597 Energy 96; 377-389
- 598 [45] Toledo F. J, Blanes J. M, (2016). Analytical and quasi-explicit four arbitrary point method  
599 for extraction of solar cell single-diode model parameters. Renewable Energy 92; 346-356.
- 600 [46] Chellaswamy C, Ramesh R, (2016). Parameter extraction of solar cell models based on  
601 adaptive differential evolution algorithm. Renewable Energy 97; 823837
- 602 [47] King D. L, Kratochvil J. A, and Boyson W. E, "Temperature coefficients for PV modules  
603 and arrays: Measurement methods, difficulties, and results," in Proc. IEEE Photovoltaic.  
604 Spec. Conf., 1997, pp. 1183–1186.
- 605 [48] KD210GH-2PU High Efficiency Multi-crystalline Photovoltaic Module Datasheet.  
606 Kyocera.(2009).[Online].Available:[http://www.kyocerasolar.de/index/products/download/  
607 English.cps\\_7724\\_files\\_8653File.cpsdownload.tmp/KD210GH2PU\\_Eng\\_January%202009  
608 .pdf](http://www.kyocerasolar.de/index/products/download/English.cps_7724_files_8653File.cpsdownload.tmp/KD210GH2PU_Eng_January%202009.pdf)
- 609 [49] SP70 Photovoltaic Solar Module Datasheet. Shell Solar. [Online]. Available:  
610 [http://telemetryhelp.com/Datasheets/ShellSP70\\_USv1.pdf](http://telemetryhelp.com/Datasheets/ShellSP70_USv1.pdf)
- 611 [50] SP85-P/80-P Solar Modules for Off Grids Markets Datasheet. Shell Solar. (2004).  
612 [Online]. Available: <http://www.effectivesolar.com/PDF/shell/SQ-80-85-P.pdf>.



Table 4: Parameters setup for considered PSO algorithm

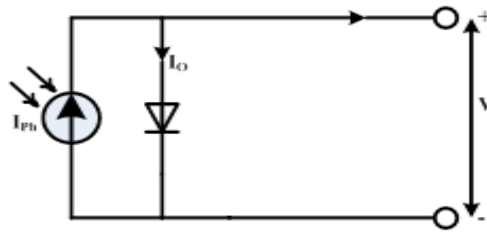
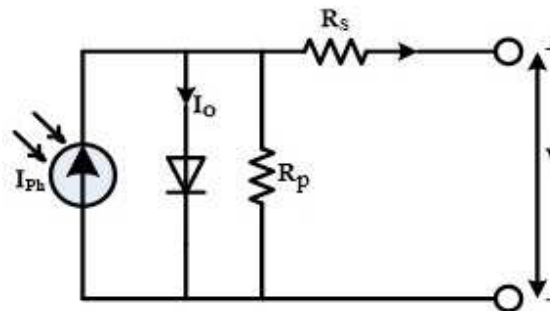
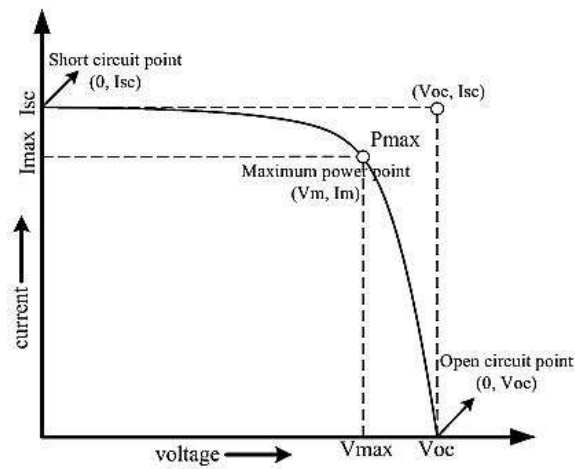
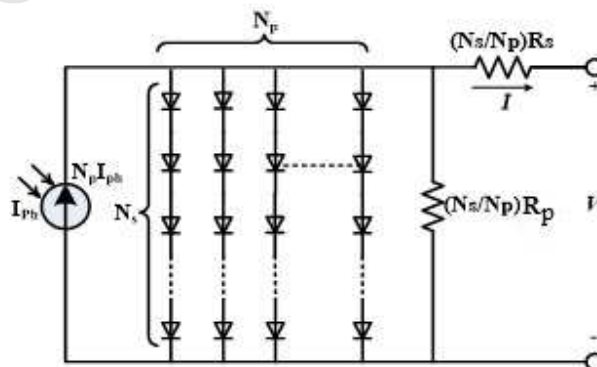
S.No.	Parameters	Values
1.	Population size ( $ps$ )	60
2.	Acceleration coefficients ( $c_1=c_2$ )	2.0
3.	Minimum value of inertia factor, ( $\omega_{min}$ )	0.4
4.	Maximum value of inertia factor, ( $\omega_{max}$ )	0.9
5.	Maximum iteration	1000
6.	Maximum tolerance for objective function	$10^{-8}$

Table 5: Identified parameters for KD210GH-2PU and SQ85 PV modules

Temperature	Values	KYOCERA-KD210GH-2PU			SHELL-SQ85		
		a	$R_s$ ( $\Omega$ )	$R_p$ ( $\Omega$ )	a	$R_s$ ( $\Omega$ )	$R_p$ ( $\Omega$ )
25 <sup>0</sup> C	Best Value ( $G_{best}$ )	1.6016	0.0012	104.5979	1.6056	0.0284	55.7392
	Mean Value ( $G_{mean}$ )	1.4809	0.0909	142.7663	1.5603	0.2161	130.1744
	Worst Value ( $G_{worst}$ )	0.6785	0.4989	193.9616	0.9177	0.5473	193.6260
50 <sup>0</sup> C	Best Value ( $G_{best}$ )	1.5996	0.0010	199.9060	1.5998	0.0010	199.9962
	Mean Value ( $G_{mean}$ )	1.5582	0.0186	165.0791	1.5448	0.0309	181.9622
	Worst Value ( $G_{worst}$ )	0.5577	0.4393	107.2338	0.6785	0.4989	193.9616
75 <sup>0</sup> C	Best Value ( $G_{best}$ )	1.5996	0.0010	199.9773	1.5998	0.0009	199.9274
	Mean Value ( $G_{mean}$ )	1.5793	0.0099	158.1982	1.5726	0.0160	171.7543
	Worst Value ( $G_{worst}$ )	0.5517	0.4393	107.2338	0.6786	0.4988	193.9616

Table 6: Comparison of absolute error at MPP (A.M 1.5, 1000 W/m<sup>2</sup>)

Method	Shell SP70				Shell SQ85			
	Mean (%)		Standard Deviation (%)		Mean (%)		Standard Deviation (%)	
	$P_{mp}$ Error	$V_{mp}$ Error	$P_{mp}$ Error	$V_{mp}$ Error	$P_{mp}$ Error	$V_{mp}$ Error	$P_{mp}$ Error	$V_{mp}$ Error
[19]	1.246	0.573	0.726	0.289	1.373	0.420	0.829	0.282
Proposed	0.003	0.068	0.002	0.045	0.001	0.077	0.002	0.047

**LIST OF FIGURES****Fig.1.** Equivalent circuit of an ideal PV model**Fig.2.** Equivalent circuit of a practical PV cell**Fig.3.** I-V characteristics curve of a PV cell.**Fig.4.** Equivalent circuit model of a PV module

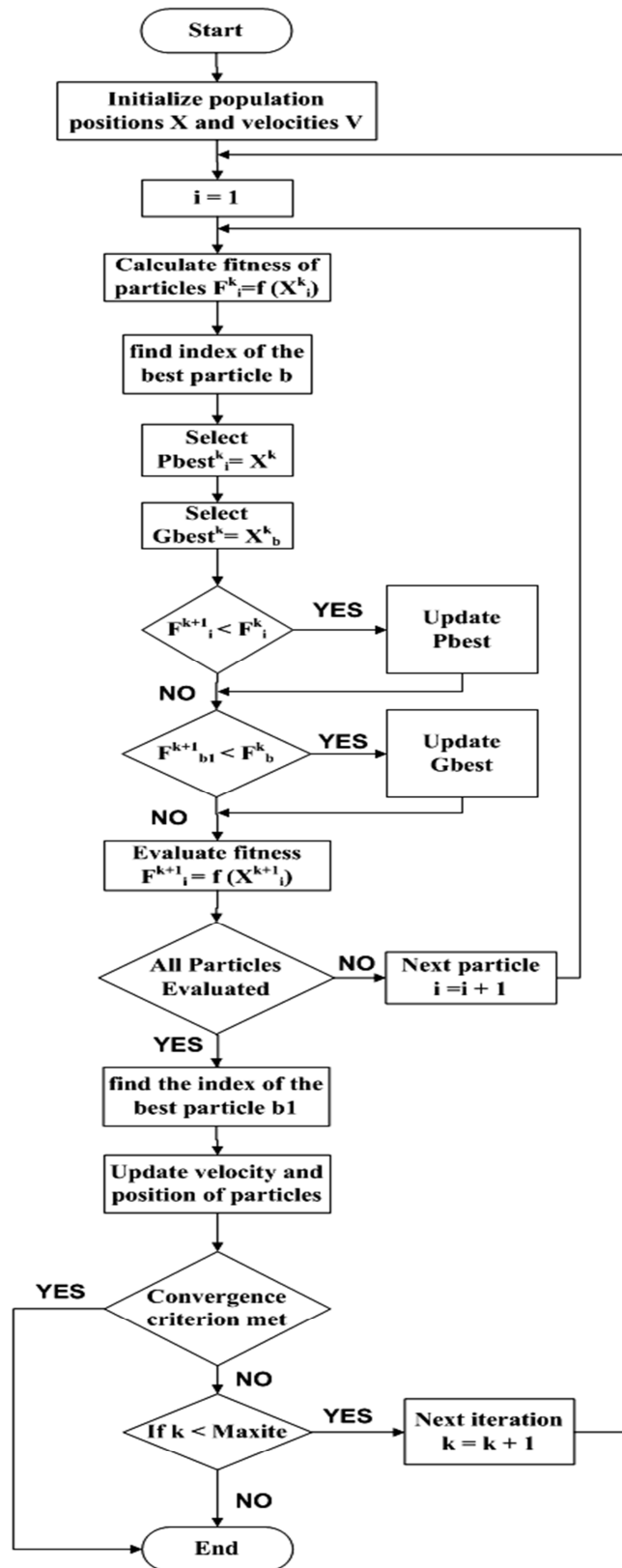


Fig.5. Flowchart of the proposed technique

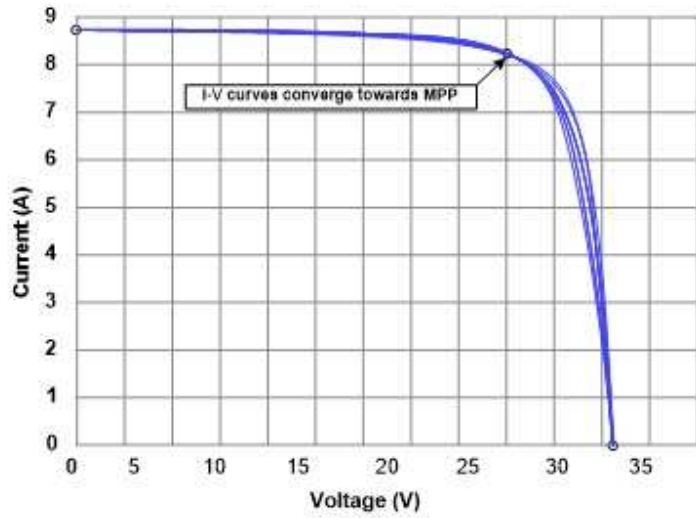


Fig.6. I-V curves obtained by the presented technique

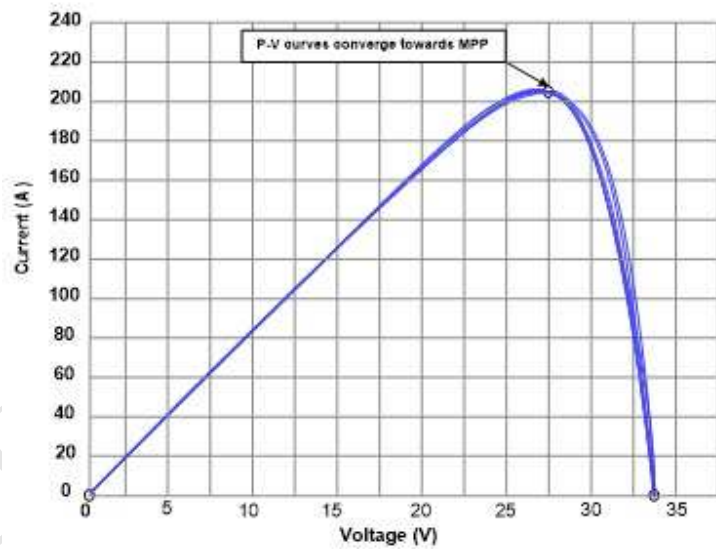


Fig.7 P-V curves obtained by the presented technique.









**HIGHLIGHTS**

- In the proposed study, unknown parameters (ideality factor, series resistance, shunt resistance) of the single diode model are identified considering binary constraints using PSO based approach.
- Based on the results of the proposed technique the characteristic curve of the PV module is validated with the manufacturer's experimental data.
- The two novel approaches have been considered as a point of reference for the proposed technique.